Universal scaling laws in surface water bodies and their zones of influence

B. S. Daya Sagar[1]

Received 30 March 2006; revised 20 July 2006; accepted 14 September 2006; published 14 February 2007.

[1] Topologically, water bodies are the first-level topographic regions that get flooded, and as the flood level gets higher, adjacent water bodies merge. The looplike network that forms along all these merging points represents zones of influence of each water body. These two topologically interdependent phenomena follow the universal scaling laws similar to certain other environmental and biological phenomena. Despite morphological variations, water bodies and their influence zones of varied sizes and shapes have different sets of scaling exponents, thereby determining that they belong to different universality classes.

Citation: Sagar, B. S. D. (2007), Universal scaling laws in surface water bodies and their zones of influence, *Water Resour. Res.*, *43*, W02416, doi:10.1029/2006WR005075.

1. Introduction

[2] The organization of the terrain is usually explained by topologically significant loopless (channel), looplike (subwatershed boundaries) networks [*Mandelbrot*, 1982; *Turcotte*, 1997; *Rodriguez-Iturbe and Rinaldo*, 1997; *Rinaldo et al.*, 2006], and the spatial distribution of water bodies.

[3] Seed and the pulp that forms around the seed are the examples of subsets of sets. Other examples include, to name a few, skeleton-body, river network–basin, grain-pore, and water body–watershed. One such phenomenon from the geophysical context is small water bodies (subsets) and their influence zones (sets). Within a biogeographic boundary, the influence of water body (M) extends to its floodwater front stagnant line, in other words zone of influence (X), the boundaries of that would be found along topographically convex zones that are attributes of various environmental and ecological geomorphologic phenomena. As illustrated schematically in Figure 1, water bodies are contained in their corresponding influence zones.

[4] Scaling exponents of certain simulated and realistic geophysical networks are derived [e.g., *Horton*, 1945; *Langbein*, 1947; *Hurst*, 1951; *Hack*, 1957; *Mandelbrot*, 1982; *Mesa and Gupta*, 1987; *Robert and Roy*, 1990; *Rosso et al.*, 1991; *Ijjasz-Vasquez et al.*, 1993; *Sagar and Rao*, 1995; *Maritan et al.*, 1996a, 1996b; *Rodriguez-Iturbe and Rinaldo*, 1997; *Banavar et al.*, 1999; *Dodds and Rothman*, 1999; *Veitzer and Gupta*, 2000; *Sagar*, 2000; *Maritan et al.*, 2002; *Sagar and Srinivas*, 2002; *Sagar and Tien*, 2004; *Sagar and Chockalingam*, 2004; *Chockalingam and Sagar*, 2005; *Tay et al.*, 2006]. These scaling exponents are derived between many morphometric parameters estimated on the basis of the analysis of geomorphologic/geophysical data available in numerous synthetic and realistic geophysical networks and basins.

[5] Water bodies, considered as local minima zones or depressions, do have characteristic shapes, sizes, and lengths that may be linked with their zones of influence or potentially flooded areas [*Sagar*, 2005]. Water bodies and their zones of influence have not been sufficiently studied yet from the viewpoint of their' scaling laws. No attempt has been made to relate the scaling exponents of these two phenomena. The goal of this paper is to derive the scaling laws (as they would reveal shared principles underlying geomorphic organization of different terrains for these two interconnected topological phenomena) via allometric relationships and certain size distributions of both water bodies and associated influence zones. The purpose of this paper is to present power laws for the organizations of water bodies and the associated influence zones, as comparing these two phenomena (like subset and set respectively to each other) by searching homogeneties is of fundamental importance. In the subsection that follows, I discuss the specifications of study region, and criteria followed in generating the zones of influence that allows the comparison of realistic water bodies and their zones of influence.

[6] I consider a region, consisting of a large number of semiartificial irrigation tanks of various sizes and shapes, of a floodplain region of Gosthani River (one of the east flowing rivers of India) situated between 18°00′ and 18°15′N latitudes and 83°15′ and 83°30′E longitudes. These water bodies are controlled by topography, and at one side minor bunds are constructed in order to store the water.

[7] The general spatial patterns of these water bodies are uniquely determined by general river flow patterns within a floodplain region. The slope of this floodplain region in general is with <2°, in which the topographic undulations are not too rough to discard the assumption of flood propagation is rather isotropic. The water bodies, from Landsat and System 1′ pour Observation de la Terre (SPOT) Geocoded visual (paper) products acquired in 1986 and 1990, are not very conspicuous. This is because the water bodies are rather (1) shallow and (2) polluted with acute siltation problem. For decades, no attempts have been made to desilt these water bodies. For these two reasons, extrac-

[1]Faculty of Engineering and Technology, Multimedia University, Melaka, Malaysia.

0043-1397/07/2006WR005075$09.00

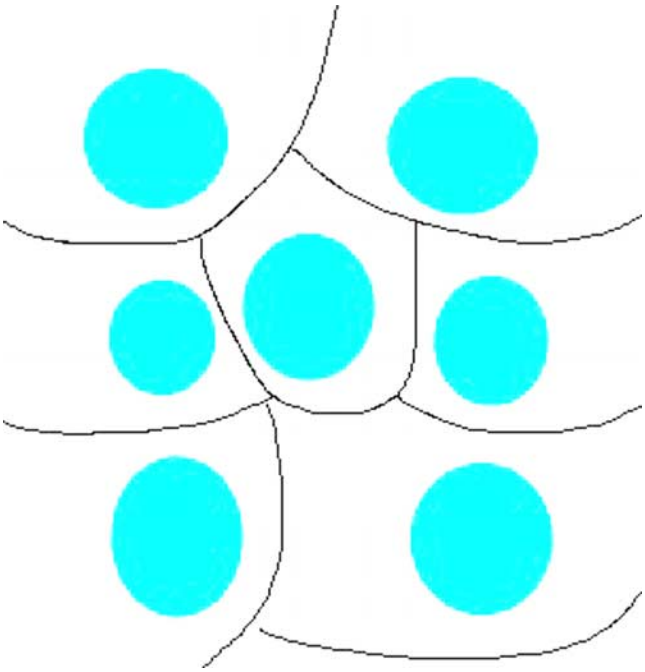

Figure 1. Schematic section diagram showing that the water bodies (cyan regions) are smaller than the influence zones (regions within the black boundaries).

tion/tracing of these water bodies directly from remotely sensed data is an arduous task.

[8] The water body data (Figures 2a and 3a) in binary format is obtained in the following way: The topographic map has been employed to trace the water bodies (with reference to the supporting remotely sensed data), the boundaries of which are given at full-tank level. With reference to topographic map source (Survey of India, toposheet), water bodies' general structures could be identified from SPOT and Landsat data. The water bodies from this topographic map are traced manually. This traced water bodies that is noise free is scanned via digital scanner in binary mode. This scanned version has been directly used for other analysis reported in the forthcoming sections. As the aim of this paper is to derive the scaling relationships via allometries and size distributions, emphasis is not laid on extraction of water bodies from remotely sensed data.

[9] The zone of influence is akin to the partitioned catchment. Usually this type of catchment divide would be extracted from analysis of DEMs [e.g., *Band*, 1986; *Vincent and Soille*, 1990]. However, because the floodplain regions are usually flat with $<2^\circ$ slope, it is difficult to derive the lines partitioning the adjacent catchments for which the water bodies (Figure 3a) act as minima. In other words, the topographic variations are too negligible to be captured from available topographic maps. Hence the impact of topography is left out while derivation of zones of influence. The study region here is obviously with $<2^\circ$. Because of the nature of the region, which is, in general, free of topographic undulations (with the exception of a few isolated hummocks of rather gently sloped hills), the assumption that the flood fills the no-water-body region in a way equivalent to morphological dilation that I adapted in derivation of zones of influence (ZIs).

[10] In the present paper, in that the aim and focus are on derivation of scaling laws of water bodies and their corresponding zones that are potentially flooded areas, I considered the following: (1) a large number of water bodies and their influence zones (the latter phenomenon is derived by following simple flood simulation principle); (2) estimated basic measures, such as areas (A), longitudinal ($L_{\|}$) and transverse lengths ($L_{\perp}$)), of both water bodies and their corresponding zones of influence; and (3) size-distributed water bodies and zones of influence.

[11] By considering the above data, finally allometric power law relations are derived on the basis of the scaling relationships between the basic measures and also on the basis of size-distributed water bodies' and zones' statistics. These derived relationships among many parameters retrieved from water bodies and ZIs can account for the power laws and provide the basis for new insights.

[12] The organization of this paper is as follows: (1) The basic morphological tools required to generate influence zones of water bodies and to perform size distributions of both water bodies and associated influence zones are briefly described in section 2. (2) Allometry-based scaling relationships of water bodies, found along topographically concave zones, and their zones of influence are given in section 3. (3) Size-distribution-based relationships for these two associated phenomena are provided in section 4. Section 5 concludes this paper with certain new insights.

2. Methods

[13] I organize this section as follows: (1) implementation of basic binary morphological transformations, (2) methodology adopted to generate zones of influence of surface water bodies, and (3) sifting of both water bodies and associated ZIs according to their sizes.

2.1. Basic Mathematical Morphological Transformations and Their Implementation

[14] Consider the set M of the water bodies, and the disk $rB(x)$ of radius r centered at point x. Dilation of M can be obtained by replacing each point m of the set M by the disk $rB(x)$, and take the union $\delta(M)$ of the results:

$$\delta(M) = \cup\{rB(m), m \in M\}, \tag{1}$$

where $\delta(M)$ is called the dilation of M by B and B be a flat structuring template, that is, a finite connected subset of discrete plane Z^2. Similarly, replace each $rB(m)$ which is included in M by its center m, and take the union $\varepsilon(M)$ of the results:

$$\varepsilon(M) = \cup\{m : rB(m) \subseteq M\}, \tag{2}$$

where the set $\varepsilon(M)$ is called the eroded set M by B. We henceforth denote set consists of water body as M in Z^2: the set complement M^c denotes the no-water-body region. For notational simplicity, I henceforth denote $\delta_B(M)$ and $\varepsilon_B(M)$ respectively as $M \oplus B$ and $M \ominus B$. The increase in radius of B is shown for n times (equation (3)). In other words, in Euclidean discrete space Z^n, nB set similar to B by factor $n = 0, 1, 2, \ldots, N$. An octagonal shaped symmetric B of primitive size 5×5 is considered to be of "size 1." The B of

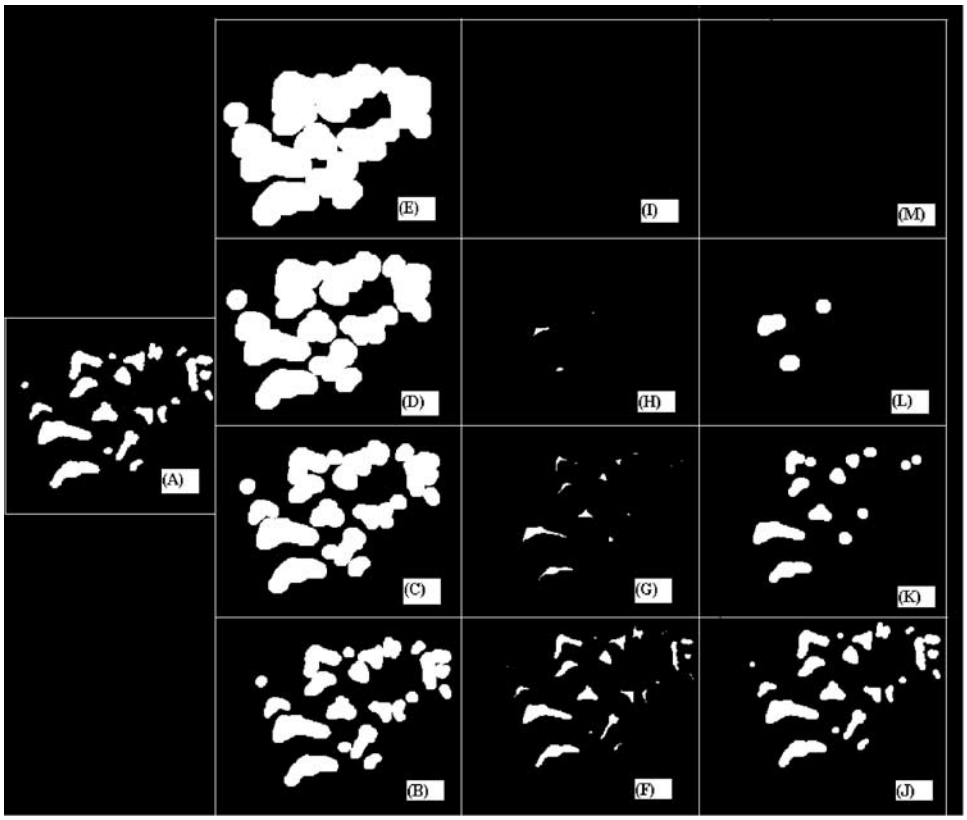

Figure 2. Illustrations of section of water body data after different degrees of morphological transformation. (a) Part of the water body data shown in Figure 3a, (b–e) increasing degrees of dilation transformation applied with increasing radius on Figure 2a, and (f–i) different degrees of erosion transformation applied on Figure 2a. Specifically, the water bodies have vanished under the erosion after the fourth cycle. (j–m) Water bodies shown in Figure 2a progressively filtered according to their sizes under the multiscale-opening transformation. The dilation (Figures 2b–2e), erosion (Figures 2f–2i), and vanishing of water bodies (Figures 2j–2m) are obvious. It is obvious that water bodies of all sizes are filtered out after the fourth cycle of opening transformation. A structuring element of primitive size 5×5, octagonal in shape, and with center as origin has been employed in this transformation.

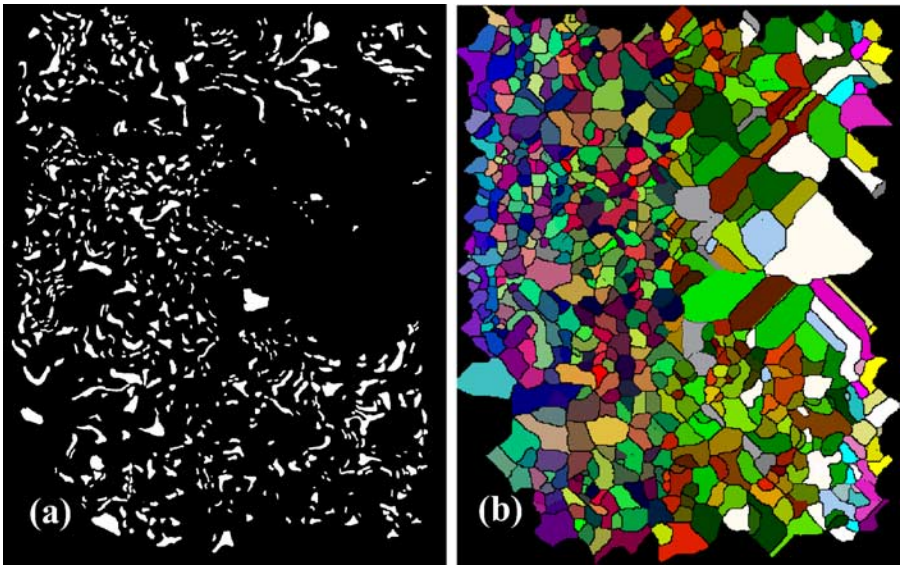

Figure 3. (a) A section consisting of a large number of small water bodies traced from the floodplain region of Gosthani River and (b) zones of influence of water bodies shown in Figure 3a. Different colors are used to distinguish the adjacent influence zones.

"size 1" denoted as "nB," is defined as Minkowski sum of B with itself n times (equation (3)). If B is of size 1, the finite sets

$$nB = \underbrace{B \oplus B \oplus B \oplus \cdots \oplus B \oplus B}_{n-times} \tag{3}$$

define a family of structuring element generated by B and parameterized by the discrete size parameter $n = 0, 1, 2, \ldots, N$. By convention, $nB = \{(0,0)\}$ if $n = 0$; $nB + mB = (n + m)B$ for any set B and for any nonnegative integers m and n. If B is convex, then nB is shaped like B but has size "n." The shape of nB is controlled by the shape of primitive size of B, whereas n controls the size. This concept of discrete shape-size family of template is due to *Lantuejoul* [1978] and *Maragos* [1989]. To generate varied degrees of dilation (erosion) effects, instead of using a larger B, with a smaller B repeatedly used to get the same effect. By increasing the radius, one can perform these dilation and erosion operations at multiple scales. Dilation (respectively the erosion) of set M by nB reduces to n dilations by symmetric element B. N iterations act as magnification factor. In turn, recursive dilations and erosions can be performed by increasing the size of the B recursively as $M \oplus nB$ and $M \ominus nB$. The properties of these two generic transformations imply that (1) neighboring water bodies merge under iterative dilations and (2) clustered water bodies will be disconnected during iterative erosions. Conversely, opening transformation is defined as erosion of the set M by B followed by dilation of eroded set (equation (4)).

$$M \circ nB = (M \ominus nB) \oplus nB \tag{4}$$

M *(or* X*)* $\circ\, nB$ eliminates from sets M or X, all water bodies or ZIs of size $<n$ (with respect to B) that is water bodies or ZIs inside which nB cannot fit. Figure 2 depicts these basic morphological transformations at respective iterations for better comprehension.

2.2. Derivation of Zones of Influence

[15] The zones within the closed stagnant boundary are termed as influence zones. The effect of iterative dilations is analogous to uniformly flooding water bodies from which after sometime we achieve floodwater-extinguishing points, through the combination of which forms ZI map. To derive zones of influence (ZI), dilation transformation, which mimics the flooding propagates from water bodies, can be recursively performed to find out the stagnant points of floodwater fronts coming from different water bodies that extinguish. This is mathematically shown in equation (5) by following skeletonization operation [*Lantuejoul*, 1978]. The zones of influence derivation part has been explained via skeletonization of M^c (set complement) to show the effect of recursive dilations to extract the stagnant boundary between floodwater fronts.

$$ZI_n(M) = \{(M^c \ominus nB) \setminus [(M^c \ominus nB) \circ B]\} \qquad n = 0, 1, 2, \ldots, N \tag{5}$$

$$ZI(M) = \bigcup_{n=0}^{N} ZI_n(M) \tag{6}$$

where the nth-level subsets of influence zones denoted by $ZI_n(M)$ are obtained by subtracting the opened version of the nth-level eroded set complement $(M)^c$ from the nth-level eroded set complement (equation (5)). Finally, the union of all the influence zone subsets (equation (6)) isolates for all $n = 0,1,2,\ldots, N$ results the boundary of zones of influence of water bodies. The limit size for recursive erosions indexed with N denotes the maximum number of iterations by octagonal element B after which, a further erosion erodes M^c down to the empty set. This implies that $N = \max\{n:(M^c \ominus nB) \neq \emptyset\}$ such that $(M^c \ominus (n + 1)B) = \emptyset$, for all $n > N$.

[16] Further, on the basis of equations (5) and (6), I construct zones of influence (X) (Figure 3b) of water bodies (M). To avoid spurious open-ended branches in the well-connected, stagnant boundary obtained by equations (5) and (6), zones of influence, a fully automated thinning operation [e.g., *Serra*, 1982; *Tay et al.*, 2006] may be performed. However, in the present paper, spurious open-ended branches are interactively removed. The regions embedded within the ZIs that also contain the associated water bodies are referred henceforth to avoid notational complexity as set X of the zones of influence. The water bodies and ZIs that exist along the sides and corners and their corresponding zones of influence are not taken into account.

2.3. Sifting of Water Bodies and Associated Zones of Influence via Multiscale Opening

[17] To sift water bodies and ZIs, multiscale opening is carried out n times (n being the radius of structuring element or the cycle number of transformation), in other words cascade of erosion-dilation of varied degrees is used to filter the water bodies (and ZIs) smaller than the nB, which is employed to distribute water bodies and ZIs according to sizes. By producing structuring elements of increasing radii, B, $2B$, $3B$, …, NB, we obtain a sequence of $(M(\text{or})X < B)$, $(M(\text{or})X < 2B)$, $(M(\text{or})X < 3B)$, …, $(M(\text{or})X < NB)$ representing the water bodies (and influence zones) respectively smaller than B, $2B$, $3B$,…, NB. To distribute the water bodies according to water bodies' size, following multiscale-opening transformation has been employed and the corresponding equation is explained.

$$\ldots \subseteq [M \circ (n + 1)B] \subseteq [M \circ nB] \subseteq \ldots \subseteq M \tag{7}$$

In the above equation, areas of (M o nB) decrease as n increases. Similarly, multiscale-opening transformation has been implemented on set X containing the associated influence zones to distribute them according to sizes. Since M and X are finite, there are positive integers $N = \max\{n: (M\,(\text{or}\,X) \ominus nB) \neq \emptyset\}$ such that $(M\,(\text{or}\,X) \ominus (n + 1)B) = \emptyset$, for all $n > N$.

[18] For the present case study, the integer N respectively for M and X include 9 and 33 cycles. This variation is because zones of influence act like sets of corresponding subsets i.e., water bodies.

[19] The information given in sections 2.1 and 2.2 are essential to derive the zones of influence of associated water bodies. After obtaining the zones of influence (Figure 3b) from the water body data (Figure 3a), I computed (1) the basic measures of both water bodies and associated influence zones and (2) certain statistical parameters from size-distributed water bodies and ZIs. However, the analysis that

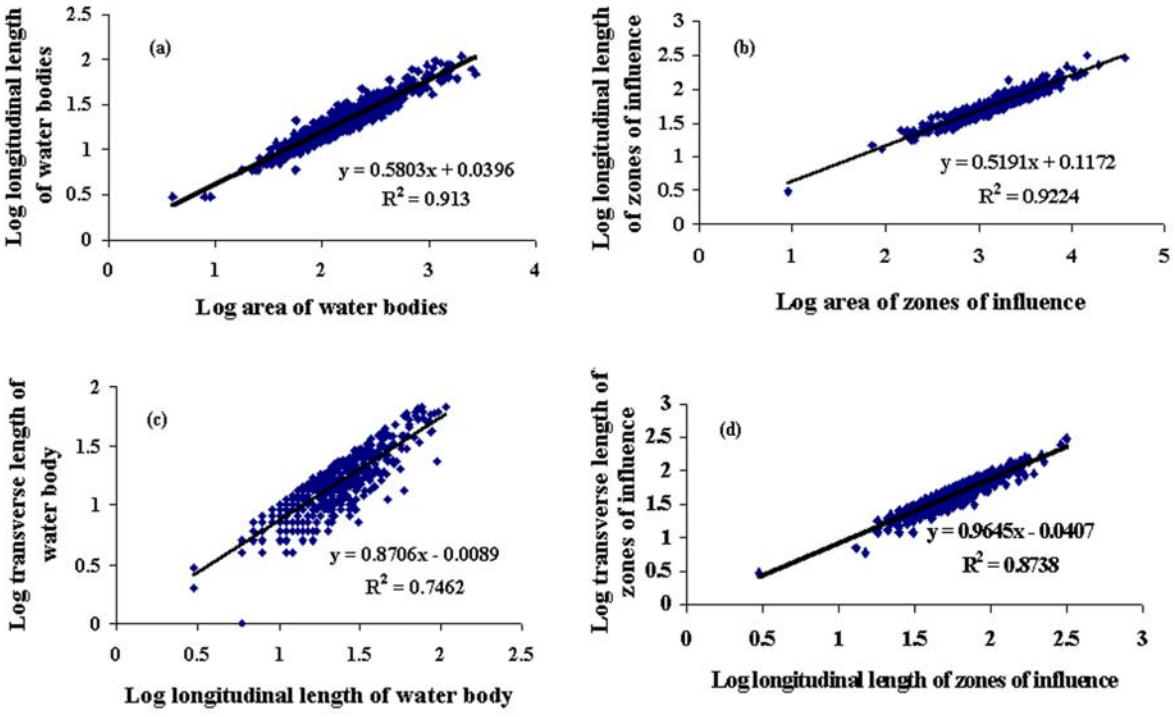

Figure 4. Allometric power law relationships: (a and b) length-area for water bodies and their zones of influence and (c and d) transverse length–longitudinal length.

follows this section relies on these basic measurements of these two associated phenomena.

3. Allometry-Based Scaling Laws

[20] By employing basic measures (Table S1 and Figures S1a and S1b of the auxiliary material[1]) such as area (A), longitudinal length ($L_{\|}$) and transverse length ($L_{\perp}$) of each water body and its corresponding influence zone, several allometric relationships (Figures 4a–4d) are derived, and find that these scaling exponents are universal type (Table 1). In Figures 4a and 4b, I show plots of A as a function of $L_{\|}$ for water bodies and their zones of influence. Remarkably, for both water bodies and their zones of influence, I find a power law scaling of the form $L_{\|} \sim A^{h}$ with exponents respectively 0.58 and 0.52 (Figures 4a and 4b). Similarly, in Figures 4c and 4d, I plot $L_{\perp}$ as a function of $L_{\|}$ for both water bodies and their zones of influence. I find H ($L_{\perp} \sim L_{\|}^{H}$) exponents of 0.87 and 0.96 respectively for water bodies and zones of influence indicating relatively smaller h ($A \sim L_{\|}^{h}$) exponent of 0.52 for zones of influence, and higher exponent of 0.58 for water bodies. This comparison further supports the notion that the higher the degree of self-affinity the lower is the exponent in the length-area relationship. These relations yield the respective exponents h and H of 0.58 and 0.87 for water bodies and 0.52 and 0.96 for the zones of water body influence. Within all categories of water bodies, the size bears a specific relationship to its zone of influence. I find that the (1) water bodies that are subsets of their zones of influence possess higher values of h than their zones of influence and (2) water bodies possess lesser values of H than their zones of influence.

[21] These two general observations are valid as larger objects (such as zones of influence) when compared to their subsets (i.e., water bodies) have a larger degree of self-affinity. It is worth mentioning here that the majority of water bodies have larger elongation ratios. These power law exponents are universal type as they possess identical scaling exponents at all scales as exhibited in certain realistic and simulated environmental phenomena [e.g., *Hurst*, 1951; *Hack*, 1957; *Mesa and Gupta*, 1987; *Robert and Roy*, 1990; *Rosso et al.*, 1991; *Ijjasz-Vasquez et al.*, 1993; *Sagar and Rao*, 1995; *Maritan et al.*, 1996a, 1996b; *Rodriguez-Iturbe and Rinaldo*, 1997; *Banavar et al.*, 1999; *Veitzer and Gupta*, 2000; *Maritan et al.*, 2002; *Sagar and Tien*, 2004] (in these studies, transverse and longitudinal lengths of realistic and model river basins are considered). Table 1 compares our estimates with allometric power laws known from other environmental geoscientific, biological and ecological contexts. Quantitative comparison with other geomorphologic systems is particularly revealing. The scaling relationships for both water bodies and their zones of influence between the h and H exponents are in accord with the results reported by other researchers [*Rodriguez-Iturbe and Rinaldo*, 1997; *Maritan et al.*, 1996a, 1996b; *Banavar et al.*, 1999; *Dodds and Rothman*, 1999; *Veitzer and Gupta*, 2000; *Maritan et al.*, 2002]. It is interesting to note the significant deviations in the scaling laws for river basins from the lower bound $1 + 2h/(1 + H) = 3/2$ [*Veitzer and*

[1]Auxiliary material data sets are available at ftp://ftp.agu.org/apend/wr/2006wr005075. Other auxiliary material files are in the HTML.

Table 1. Comparative Scaling Relationships

System	h	H	$\alpha = 1 + h$	$h = \frac{1}{1+H}$	$1 + \frac{2h}{1+H}$	A versus N
Water bodies	0.60	0.86	1.60	0.54	1.64	1.41
Zones of influence	0.56	0.94	1.56	0.52	1.57	1.70
OCN (rectangular boundary)[a]	0.57	0.84	1.57	0.54	1.57	–
OCN (fractal boundary)[a]	0.56	0.88	1.56	0.53	1.56	–
F-SCN[b]	0.55	0.95	0.55	0.52	1.54	–

[a]Optimal channel network.
[b]Fractal skeletal based channel network. Source: *Sagar et al.* [1998].

Gupta, 2000]. On the basis of these two exponents, the following interesting observations are noted:

[22] 1. Relationship of $h = 1/(1 + H)$ is very well fitted for the water bodies and their zones of influence, which further indicates that these two interrelated topologic phenomena are self-affine as $H < 1$ (Table 1).

[23] 2. Estimates for $1 + 2h/(1 + H)$ yield 1.64 and 1.57 respectively for water bodies and their zones of influence supporting the scaling relationship with exponent larger than 3/2.

[24] 3. A quantity $\alpha = 1 + h$, originally derived on the basis of the allometric scaling relationship of mass-basin metabolic rate [*Maritan et al.*, 2002], for water bodies and their zones of influence respectively yields 1.60 and 1.56.

[25] 4. Results further indicate that the degree of preserving geometric similarity is more in zones of influence than in their corresponding water bodies. This may be attributed to the fact that the exogenically sensitive water bodies have larger elongation ratio.

[26] 5. Relationships between h_M and h_X, and H_M and H_X (Figures 5a and 5b), however, yield low goodness of fit.

[27] 6. Dependency of water body size on ZI size yields a power law relationship with exponent 0.58 implying a relationship with slope 3/5 (Figure 5c).

[28] 7. The reason for having no correlation between the h, H exponents of water bodies and associated zones of influence (Figures 5a and 5b) is because there is no linear relationship observed between the areas of water bodies and their ZIs (Figure 5c). This further implies that the sizes of the ZIs are not dependent on water bodies' sizes. Hence it could not be generalized that the smaller water bodies have smaller ZIs (or) larger water bodies have larger ZIs. This discrepancy may be attributed to the following fact: within the data considered, there are several regions with sparsely populated water bodies (both small- and large-size categories). In such regions, the ZIs of corresponding water bodies with sparse population evidently occupy more area. This is not true in the regions where the water bodies' population is denser. Perhaps, proper correlation may be observed, if one considers the region with rather homogeneously populated water bodies.

[29] In this section, the relationships derived are essentially based on the measurements based on the areal and linear aspects of water bodies and ZIs of all size categories. However, in the section that follows, I show relationships between the size-distributed water bodies and ZIs, and scale imposed because of varied sizes of structuring element.

4. Size-Distribution-Based Scaling Laws

[30] I perform multiscale opening [*Serra*, 1982] (see section 2.3) to sift the water bodies (Figure 3a) (and their ZIs (Figure 3b)) that are smaller than the template by leaving larger water bodies (and ZIs). I perform this sifting recursively until the sections (Figures 3a and 3b) become empty. I distinguish portions of M and X by sifting them according to their sizes (see section 2.3). Number (N) and contributing area (A) of the retained water bodies (N_M, A_M) and their ZIs (N_X, A_X) after each cycle of opening transfor-

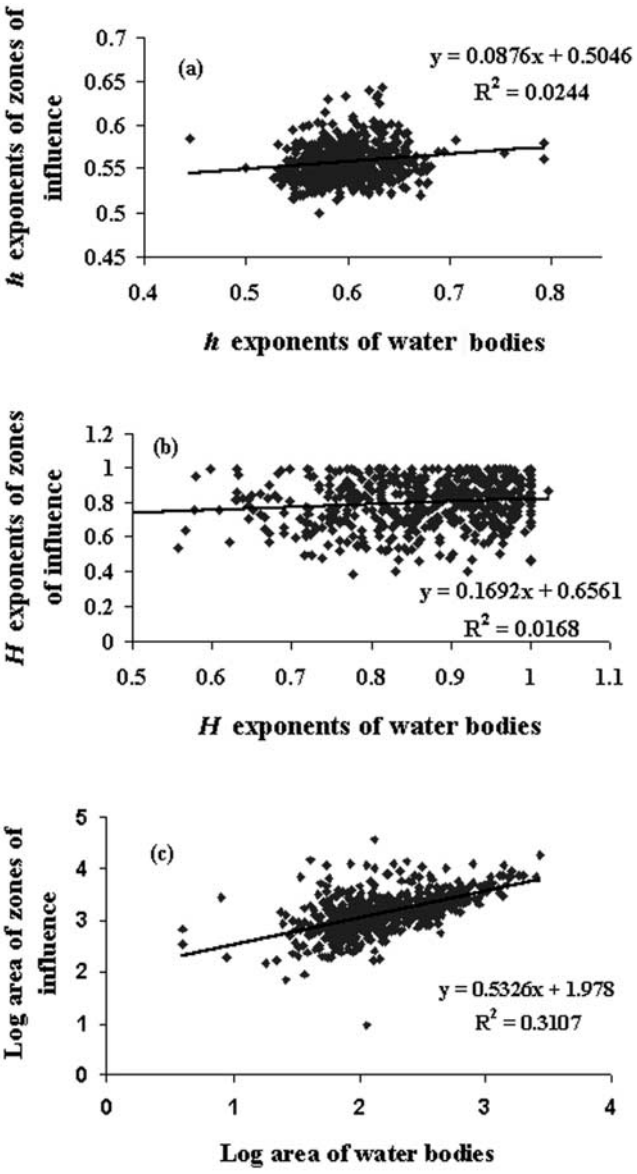

Figure 5. (a) Hack's exponents, (b) Hurst exponents of water bodies and their zones of influence, and (c) areas of water bodies and ZIs.

Table 2. Areas and Number of Surface Water Bodies and Their Zones of Influence After Respective Degree of Sifting[a]

Cycle	Structuring Element Size	Area of Water Bodies (and ZIs)[b]	Number of Water Bodies (and ZIs)
0	0	163,783 (1,234,566)	645 (645)
1	5	155,250 (1,213,515)	580 (621)
2	9	100,909 (1,171,792)	288 (620)
3	13	54,807 (1,127,634)	121 (587)
4	17	28,581 (1,061,809)	41 (523)
5	21	15,989 (976,057)	15 (445)
6	25	12,218 (871,559)	10 (367)
7	29	6801 (752,042)	6 (330)
8	33	4643 (632,944)	3 (225)
9	37	1358 (523,085)	1 (152)
10	41	0 (442,187)	0 (109)
11	45	0 (369,017)	0 (84)
12	49	0 (313,898)	0 (65)
13	53	0 (284,865)	0 (62)
14	57	0 (239,058)	0 (52)
15	61	0 (194,656)	0 (33)
16	65	0 (173,284)	0 (28)
17	69	0 (157,351)	0 (24)
18	73	0 (125,092)	0 (17)
19	77	0 (112,670)	0 (15)
20	81	0 (103,365)	0 (14)
21	85	0 (76,682)	0 (10)
22	89	0 (66,530)	0 (7)
23	93	0 (65,256)	0 (6)
24	97	0 (55,234)	0 (5)
25	101	0 (43,606)	0 (2)
26	105	0 (40,588)	0 (2)
27	109	0 (29,986)	0 (1)
28	113	0 (29,710)	0 (1)
29	117	0 (29,337)	0 (1)
30	121	0 (28,951)	0 (1)
31	125	0 (28,306)	0 (1)
32	129	0 (27,449)	0 (1)
33	133	0 (26,665)	0 (1)

[a]ZIs, zones of influence.
[b]Areas are given in pixel units.

mation are computed (Table 2). I find simple scaling power law relationships between the N and A of water bodies and their zones of influence (Figures 6a and 6b) that could be sifted with increasing radius (r) of templates. For water bodies and their zones of influence:

[31] 1. The number-area-based power law relationships, supporting universality class, respectively in the form of $N_M \sim A_M^{1.41}$ and $N_X \sim A_X^{1.70}$ (Figures 6a and 6b). This relationship translates a physical phenomenon of drought under the general assumption that the smaller water bodies easily get affected by drought condition. With increasing drought conditions, water bodies of increasing size categories would be vanished. The multiscale-opening transformation mimics the impact of increasing drought. However, there may not be any significant change in the ZI power laws as its area gets least affected.

[32] 2. Results show that the power law exponent in water bodies is smaller than that of their zones of influence. This is due to fact that zones of influence act as supersets of their water bodies.

[33] Size distributions and their density functions are estimated as follows to find the extent of deviations between size categories, in terms of power law that I derived between the size of water body and its corresponding ZI. To compute the size distribution functions, normalized size and number distribution functions for water bodies and their zones of influence are derived as

$$S(k) = 1 - \left[\frac{A(M(or)X < nB)}{A(M(or)X)}\right], \tag{8}$$

where $n \in [0, N]$, numerator and denominator respectively represent sum of all the water body or ZI elements larger than the specified size of reference template (B) of size n, and total area of all the water bodies or ZIs of all size categories. Using these normalized distribution functions of both water bodies and their zones of influence, I compute the probability density function to describe the size attributes of individual water bodies and their ZIs as

$$GS(k) = [S(k+1) - S(k)] \tag{9}$$

[34] From normalized size (and number) distributions and their density functions of water bodies and corresponding zones of influence, the following observations are made: (1) Residues of M and X by removing portions smaller than the threshold template size. (2) Smaller size categories of water bodies and their influence zones relatively occupy more area, and find significant drop in surface area between two consecutive levels of siftings (Figure 6c) indicating that the region contains water bodies and influence zones of comparable size to the smaller level of sifting. (3) A local maximum in the size distribution plots (Figure 6c) that is equivalent to the first derivative of the surface area at a given scale indicates the presence of many water bodies at that scale. (4) Significant similarity is obvious in the general trends of the plots (Figure 6c) for surface water bodies and their ZIs (Table 2) indicating certain spatial relationship between these two intertwined topological phenomena; this is a generalized relationship to a joint probability density and show that fluctuations about scaling are substantial.

[35] In addition to these scaling relationships, I further extend to derive scaling laws between the correlation sums (C(r)) of areas (and number) and radius of structuring template. To compute correlation sums of areas of water bodies (and ZIs), the ratio between the area of water bodies (and ZIs) that could be filtered with a template with radius r, and the total area squared of water bodies (and ZIs) is considered and expressed as

$$\left[\frac{A\{M(or)X < rB\}}{(r^2)}\right] \tag{10}$$

[36] By replacing the areas (A) with the number (N) of isolated water bodies (and ZIs), in the above equation, correlation sums of number are computed as

$$\left[\frac{N\{M(or)X < rB\}}{(r^2)}\right] \tag{11}$$

[37] I plot graphs for size distribution and discrete first derivative functions of sizes of water bodies and their zones of influence. These relationships (Figure 7a) yield the power law exponents for water bodies (M) and their zones of influence (X) respectively for the following: area-$C(r)_M \sim (r)^{1.26}$; area-$C(r)_X \sim (r)^{1.16}$; number-$C(r)_M \sim (r)^{0.94}$; and

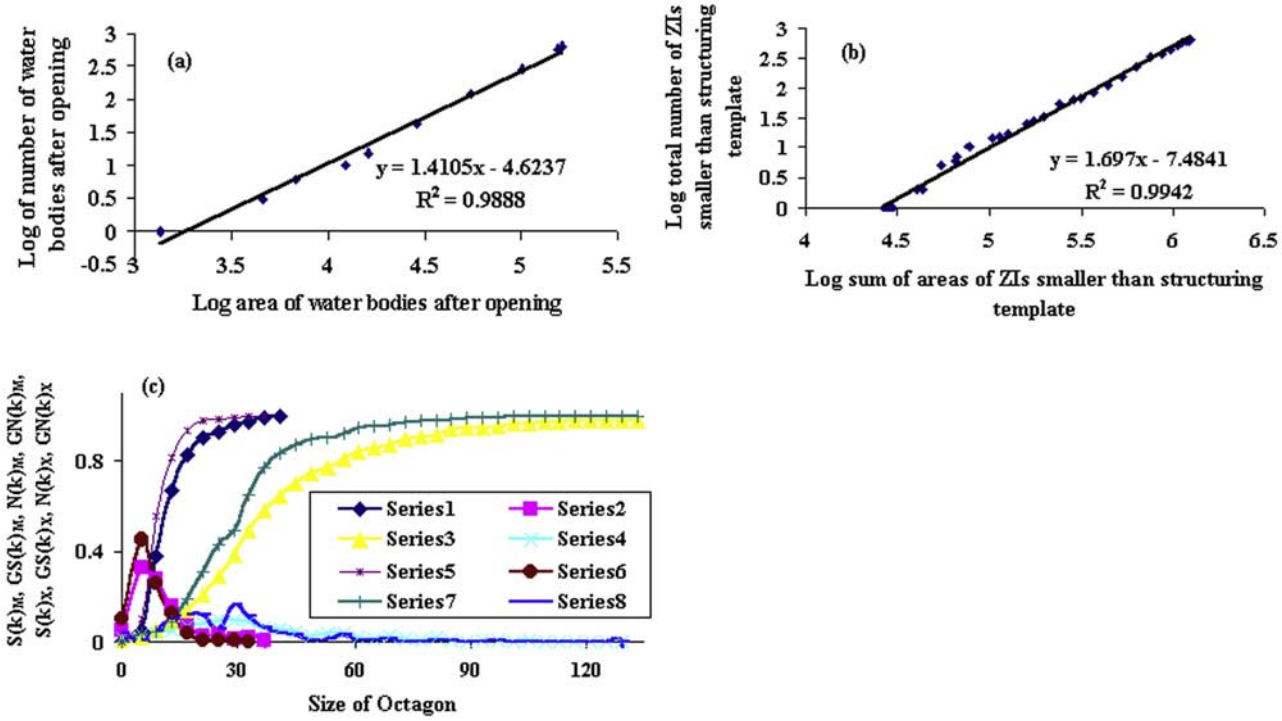

Figure 6. (a and b) Number-area relationship for water bodies and their ZIs that yield power laws of 1.41 and 1.70, respectively, and (c) normalized size and number distribution and density functions of water bodies and ZIs plotted against the size of the octagon (eight series of points). The size distribution plots give information about the size distribution of water bodies and their influence zones: approximately 50,000 pixels belong to water bodies of 5-pixel diameter, 50,000 pixels belong to water bodies of 10-pixel diameter, and 25,000 pixels belong to water bodies of 11-pixel diameter. Local maxima in the distribution spectra at a given scale indicate the presence of many water bodies and influence zones at that scale.

number-$C(r)_X \sim (r)^{1.03}$, further indicating that the number-wise distributions of both water bodies and ZIs is more homogeneous than that of the area-wise distribution. Further, a power law relationship is derived via a log-log plot between $(1/r)$, and the ratios of areas (and numbers) of water bodies and their zones of influence retained after progressive sifting by means of increasing radii of templates, and the squared radius (r^2) of the template (Figure 7b) (see the description for Figure 7b).

5. Conclusions

[38] On the basis of the results derived from allometry- and size-distribution-based power laws, which are in accordance with universal power laws, the following are inferred.

[39] 1. Power laws that can model the sizes of the influence zones are overestimated than that of associated water bodies.

[40] 2. Water bodies and associated zones of influence belong to different universality classes (Figures 4a–4d, 6a, and 6b), and further emphasize that certain scaling rules may apply to both exogenically sensitive and insensitive geomorphic phenomena.

[41] 3. Correlation is not obvious between the h, H exponents (Figures 5a and 5b) of water bodies and associated zones of influence, as there is no size-based relationship between the ZIs and water bodies (Figure 5c). This poor correlation may be attributed to the fact that, within the data considered, there are several regions with sparsely populated water bodies (both small and larger size categories). In such regions, the ZIs of corresponding water bodies with sparse population evidently occupy more area. This is not true in the regions where the water bodies' population is denser.

[42] 4. Significant results derived as power laws based on distributions (size and number) of water bodies and zones of influence via multiscale-opening transformation translate probably a physical phenomenon of drought. This relationship (Figures 6a and 6b) translates a physical phenomenon of drought under the general assumption that the smaller water bodies easily get affected by drought condition. With increasing drought conditions, exgogenically sensitive water bodies of increasing size categories would be vanished. However, there may not be any significant change in the ZI power laws as its area gets least affected by any exogenic process. It is worth monitoring the extent of deviations in the scaling laws, as one of the two phenomena is exogenically sensitive.

[43] 5. Number and areas of the size-distributed water bodies and ZIs plotted as functions of size of the structuring template employed to distribute also reveal different classes of universality characters (Figures 7a and 7b).

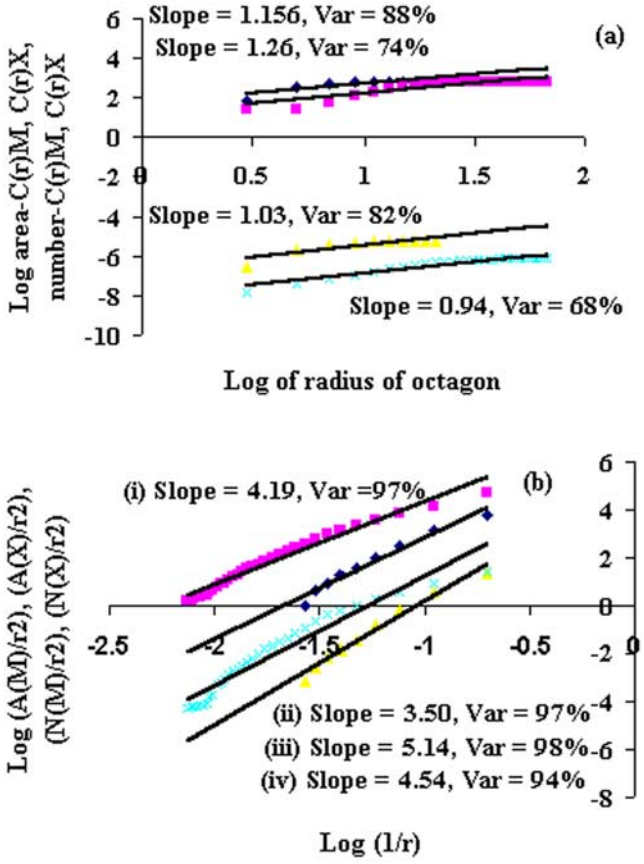

Figure 7. (a) Power law relationship between radius and area correlation sum of water bodies (yellow) and zones of influence (cyan) and number correlation sum of water bodies (blue) and zones of influence (pink). (b) Power law relationships between $(1/r)$ and the ratios of (i) $\left[\frac{A_M \le nB}{r^2}\right]$, (ii) $\left[\frac{A_X \le nB}{r^2}\right]$, (iii) $\left[\frac{N_M \le nB}{r^2}\right]$, and (iv) $\left[\frac{N_X \le nB}{r^2}\right]$.

[44] These scaling laws provide several new insights to understand the relationships between water bodies and ZIs in terms of the information about form and function. Further adherence of water bodies and their zones of influence to regular scaling rules improve our understanding in modeling and reconstruction of environmentally dependent geomorphic system processes. The derived relationships can account for scaling laws and may serve as the basis for new insights of investigations. It is hoped that scaling relationships for water bodies and their influence zones will provide a way to better understanding of paleoenvironments and their geomorphic constitutions.

Notation

Z^n	Euclidean discrete n-dimensional space.
m, x, b	points of Z^2.
M, X, B	subsets of Z^2; M is set containing water bodies, X is set containing zones of influence, $M \subseteq X$ indicates that water bodies are subsets of zones of influence.
M^c	complement of M in Z^2.
$\cup, \cap, \setminus, \subseteq$	logical union, logical intersection, logical difference, and improper subset.
$M \cup X$	union of M and X.
$M \cap X$	intersection of M and X.
$M \setminus X$	set difference of M and X.
nB	nth-size structuring element symmetric with respect to origin at center.
$1B$	primitive element with origin at center, and radius 1.
NB	largest size of structuring element.
$\oplus, \ominus$, o	symbols for dilation, erosion, and opening.
$M \oplus B = \cup_{b \in B} M_b$	morphological dilation of M with respect to B.
$\emptyset$	empty set.
n	iteration/cycle number (or radius of structuring element, where $n = 0, 1, 2, \ldots, N$).
N	maximum iteration/cycle number required transforming a set to the state of idempotence.
$A(\cdot)$	finite set of cardinality.
$L_\parallel$	longitudinal length.
$L_\perp$	transverse length.
H	exponent derived from $L_\parallel$ and $L_\perp$.
h	exponent derived from $L_\parallel$ and A.
h_M	exponent h for water bodies.
h_X	exponent h for zones of influence.
H_M	exponent H for water bodies.
H_X	exponent H for zones of influence.
N_M	number of water bodies.
A_M	area of water bodies.
N_X	number of zones of influence.
A_X	area of zones of influence.

[45] **Acknowledgments.** I thank Jayanth Banavar, Gabor Korvin, Jean Serra, and Andrea Rinaldo for their encouragement, useful comments, and suggestions. I am also thankful to Sergio Fagherazzi, Jay Gao, Andre Roy, and three anonymous reviewers, who provided several useful comments and suggestions on earlier versions of the manuscript.

References

Banavar, J. R., A. Maritan, and A. Rinaldo (1999), Size and form in efficient transportation networks, *Nature*, *399*, 130–134.

Band, L. E. (1986), Topographic partition of watersheds with digital elevation models, *Water Resour. Res.*, *22*(1), 15–24.

Chockalingam, L., and B. S. D. Sagar (2005), Morphometry of networks and non-network spaces, *J. Geophys. Res.*, *110*, B08203, doi:10.1029/2005JB003641.

Dodds, P. S., and D. H. Rothman (1999), Unified view of scaling laws for river networks, *Phys. Rev. E*, *59*, 4865–4877.

Hack, J. T. (1957), Studies of longitudinal profiles in Virginia and Maryland, *U. S. Geol. Surv. Prof. Pap.*, *294-B1*.

Horton, R. E. (1945), Erosional development of stream and their drainage basin: Hydrological approach to quantitative morphology, *Geophys. Soc. Am. Bull.*, *56*, 275–370.

Hurst, H. E. (1951), Long-term storage capacity of reservoirs, *Trans. Am. Soc. Civ. Eng.*, *116*, 770–808.

Ijjasz-Vasquez, E. J., R. L. Bras, and I. Rodriguez-Iturbe (1993), Hack's relation and optimal channel networks: The elongation of river basins as a consequence of energy minimization, *Geophys. Res. Lett.*, *20*, 1583–1586.

Langbein, W. B. (1947), Topographic characteristics of drainage basins, *U. S. Geol. Surv. Prof. Pap.*, *968-C*.

Lantuejoul, C. (1978), La squelettisation et son application aux mesures topologuiques des mosaiques polycristallines, these de Docteur-Ingenieur, Sch. of Mines, Paris.

Mandelbrot, B. (1982), *Fractal Geometry of Nature*, W. H. Freeman, New York.

Maragos, P. (1989), Pattern spectrum and multiscale representation, *IEEE Trans. Pattern Anal. Mach. Intel.*, *11*(7), 701–716.

Maritan, A., F. Coloairi, A. Flammini, M. Cieplak, and J. R. Banavar (1996a), Universality classes of optimal channel networks, *Science*, *272*, 984–988.

Maritan, A., A. Rinaldo, R. Rigon, A. Giacomatti, and I. Rodriguez-Iturbe (1996b), Scaling laws for river networks, *Phys. Rev. E*, *53*, 1510–1515.

Maritan, A., R. Rigon, J. R. Banavar, and A. Rinaldo (2002), Network allometry, *Geophys. Res. Lett.*, *29*(11), 1508, doi:10.1029/2001GL014533.

Mesa, O. J., and V. K. Gupta (1987), On the main channel length: Area relationships for channel networks, *Water Resour. Res.*, *23*, 2119–2122.

Rinaldo, A., J. R. Banavar, and A. Maritan (2006), Trees, networks, and hydrology, *Water Resour. Res.*, *42*, W06D07, doi:10.1029/2005WR004108.

Robert, A., and A. Roy (1990), On the fractal interpretation of the mainstream length-drainage area relationship, *Water Resour. Res.*, *26*, 839–842.

Rodriguez-Iturbe, I., and A. Rinaldo (1997), *Fractal River Basins: Chance and Self-Organization*, Cambridge Univ. Press, New York.

Rosso, R., B. Becchi, and P. LaBarbera (1991), Fractal relation of main stream length to catchment area in river networks, *Water Resour. Res.*, *27*, 381–387.

Sagar, B. S. D. (2000), Fractal relation of medial axis length to the water body area, *Discrete Dyn. Nature Soc.*, *4*, 97.

Sagar, B. S. D. (2005), Discrete simulations of spatio-temporal dynamics of small water bodies under varied streamflow discharges, *Nonlinear Processes Geophys.*, *12*, 31–40.

Sagar, B. S. D., and L. Chockalingam (2004), Fractal dimension of non-network space of a catchment basin, *Geophys. Res. Lett.*, *31*, L12502, doi:10.1029/2004GL019749.

Sagar, B. S. D., and B. S. P. Rao (1995), Fractal relation on perimeter to the water body area, *Current Sci.*, *68*, 1129–1130.

Sagar, B. S. D., and D. Srinivas (2002), Estimation of number-area-frequency dimensions of surface water bodies, *Int. J. Remote Sens.*, *20*, 2491–2496.

Sagar, B. S. D., and T. L. Tien (2004), Allometric power-law relationships in a Hortonian fractal DEM, *Geophys. Res. Lett.*, *31*, L06501, doi:10.1029/2003GL019093.

Sagar, B. S. D., C. Omoregie, and B. S. P. Rao (1998), Morphometric relations of Fractal-skeletal based channel network model, *Discrete Dyn. Nature Soc.*, *2*, 77–92.

Serra, J. (1982), *Image Analysis and Mathematical Morphology*, Elsevier, New York.

Tay, L. T., B. S. D. Sagar, and H. T. Chuah (2006), Allometric relationships between travel-time channel networks, convex hulls, and convexity measures, *Water Resour. Res.*, *42*, W06502, doi:10.1029/2005WR004092.

Turcotte, D. L. (1997), *Fractals and Chaos in Geology and Geophysics*, Cambridge Univ. Press, New York.

Veitzer, S. A., and V. K. Gupta (2000), Random self-similar river networks and derivations of generalized Horton laws in terms of statistical simple scaling, *Water Resour. Res.*, *36*, 1033–1048.

Vincent, L., and P. Soille (1990), Watersheds in digital spaces: An efficient algorithm based on immersion simulation, *IEEE Trans. Pattern Anal. Mach. Intel.*, *13*(6), 583–598.

B. S. D. Sagar, Faculty of Engineering and Technology, Melaka Campus, Multimedia University, Jalan Ayer Keroh Lama, 75450 Melaka, Malaysia. (bsdaya.sagar@mmu.edu.my)